Development and Optimization of a High-Throughput Bioassay for TRPM7 Ion Channel Inhibitors

BRANDI CASTILLO,[1] PETER PÖRZGEN,[1] REINHOLD PENNER,[2]
F. DAVID HORGEN,[1] and ANDREA FLEIG[2]

TRPM7 is a ubiquitously expressed and constitutively active divalent cation channel essential for cell survival and proliferation because it provides a mechanism for Mg^{2+} entry. This makes the channel an attractive target for proliferative diseases. In keeping with its role in Mg^{2+} homeostasis, TRPM7 is inhibited by intracellular Mg^{2+} and Mg-ATP. TRPM7 has been implicated in anoxia-mediated cell death following brain ischemia. Despite its critical role in ischemic cell death and cell proliferation, there are no reports of selective inhibitors of TRPM7. The authors developed and optimized a fluorescent dye-based bioassay measuring the fluorescence quench of fura-2 by TRPM7-mediated Mn^{2+} influx in HEK293 cells that stably overexpress TRPM7. The following bioassay conditions were evaluated: (a) cell density, (b) dye loading conditions, (c) bioassay temperature, (d) concentration of the fura-2 quenching agent Mn^{2+}, and (e) concentration of vehicle solvent. The bioassay was validated by measuring the effects of the known (nonselective) inhibitor 2-APB and La^{3+} on Mn^{2+} influx, and furthermore, the performance of the assay was evaluated by screening a subset of a marine bacteria-derived extract library. The quality of the bioassay window is excellent based on an established statistical parameter used to evaluate high-throughput screening window quality (Z and Z′ factors ≥0.5). (*Journal of Biomolecular Screening* 2010:498-507)

Key words: TRPM7 ion channels, high-throughput bioassay, fura-2 quench by Mn^{2+}, cell-based assay, TRPM7-HEK293 cell line, natural product library, marine bacteria

INTRODUCTION

MEMBERS OF THE TRANSIENT RECEPTOR POTENTIAL (TRP) ion channel superfamily are grouped by their homology and exhibit considerable variation in their physiological functions. However, most TRP channels are permeable to Ca^{2+},[1] an important mediator of many cellular events, and play various roles in sensory transduction.[2] Several mammalian TRP channels have been validated or are emerging targets for human pathologies.[3]

The seventh member of the melastatin subfamily of TRP channels (TRPM7) was discovered in 2001[4,5] as a cell entry mechanism for Mg^{2+} and other divalent cations.[4] The protein is expressed ubiquitously, with highest prevalence in the heart, pituitary, bone, and adipose tissue and significant expression in the central nervous system.[6] TRPM7 is the only known ion channel, to date, that is required for cell viability.[7] Careful regulation in the cell is critical because, in most cells studied, both overexpression and targeted deletion eventually lead to cell death.[4] The decreased viability of TRPM7-deficient cells can be overcome by Mg^{2+} supplementation, which reveals an essential role for TRPM7 in Mg^{2+} homeostasis in mammalian cells. TRPM7 is constitutively active in resting cells[4] and is regulated by $[ATP]_i$, $[ADP]_i$, and $[Mg^{2+}]_i$ with physiological levels of Mg-ATP and $[Mg^{2+}]_i$ inhibiting channel activity by 85%.[8]

TRPM7 subunits are composed of 1863 amino acids, which form 6 transmembrane domains with a pore-forming region between transmembrane segments 5 and 6. Functional TRPM7 channels demonstrate a tetrameric quaternary structure, resulting in an overall topography similar to a number of voltage-gated cation channels. TRPM7 is unique among known ion channels in its possession of a functional α-kinase domain in its C-terminal region.[4,5,9] This enzymatic domain is capable of autophosphorylation[9] and has 2 other known substrates: annexin 1[10] and myosin IIA.[11] However, the physiological function of the α-kinase domain is not fully understood. Electrophysiologically, TRPM7 is characterized as a voltage-independent divalent-selective channel whose current-voltage relationship is nonlinear and displays strong outward rectification. TRPM7 has the following selectivity profile for divalent cations: $Zn^{2+} \approx Ni^{2+} >> Ba^{2+} > Co^{2+} > Mg^{2+} \geq Mn^{2+} \geq Sr^{2+} \geq Cd^{2+} \geq Ca^{2+}$.[12]

[1]College of Natural Sciences, Hawaii Pacific University, Kaneohe, Hawaii.
[2]Center for Biomedical Research at The Queen's Medical Center and John A. Burns School of Medicine at the University of Hawaii, Honolulu, Hawaii.

Received Sep 22, 2009, and in revised form Mar 1, 2010. Accepted for publication Mar 4, 2010.

Journal of Biomolecular Screening 15(5); 2010
DOI: 10.1177/1087057110368294

Neurodegeneration caused by ischemia is thought to be triggered by a large influx of Ca^{2+} and Na^{+} as an excitatory response to high extracellular levels of glutamate following cellular energy depletion. However, it has been discovered recently that ischemia-induced increases in $[Ca^{2+}]_i$ are sustained by glutamate-independent pathways, thereby providing a rationale for the observation that antiexcitatory therapies suffer from a limited window of effectiveness.[13] TRPM7 is one of the few channels that have been demonstrated as a secondary glutamate-independent Ca^{2+} entry mechanism in ischemia models,[13,14] and the channel activity is potentiated by conditions that develop during ischemic events, including low levels of the extracellular divalents Mg^{2+} and Ca^{2+},[15] and ROS/RNS production.[13] It is quite clear by now that suppression of TRPM7 is advantageous for neuronal survival after an ischemic event in vivo.[16] Thus, inhibition of TRPM7 emerges as a promising strategy for arresting neuronal damage following an ischemic stroke and may extend the timeframe for effective treatment.

In addition to its role in ischemia, the involvement of TRPM7 in cell growth and proliferation suggests that TRPM7 could be a target in several cancers. For example, it has been reported that TRPM7 is abundantly expressed in a variety of human carcinoma cells, including gastric adenocarcinoma cells,[17] breast cancer cells,[18] and human head and neck carcinoma cells.[19] Moreover, suppression of TRPM7 by siRNA and/or nonselective inhibitors has been shown to inhibit the growth of each of these cell types. At the same time, overexpression of TRPM7 was detected in breast cancer tissues, and TRPM7 expression level correlates with their proliferative potential.[18]

Despite the significant therapeutic potential of TRPM7, there are no selective modulators reported for the channel, so far, which significantly hampers validation of TRPM7 as a drug target for stroke and cancer. Currently, a few nonselective TRPM7 inhibitors exist and have collectively proven useful in investigating the pharmacology of TRPM7 in cell-based experiments. These substances include 2-aminoethyl diphenylborinate (2-APB),[20,21] lanthanides (La^{3+} and Gd^{3+}),[13,22] carvacrol,[23] and polyamines.[24] However, each of these compounds modulates related and unrelated ion channels, greatly reducing their utility as tool compounds for advancing the understanding of TRPM7's role in physiological and pathophysiological conditions. The discovery of selective inhibitors of TRPM7 will provide valuable tool compounds for models of ischemia-reperfusion and cancer. Furthermore, such compounds may also serve as leads in the development of novel therapeutic approaches for ischemic stroke and certain cancers.

The discovery of tool compounds for the TRPM7 channel will be greatly facilitated with the development of a high-throughput screening (HTS) assay capable of detecting inhibition of TRPM7 ion channel function, yet to date, there are no reports of TRPM7 HTS assays. Although TRPM7 function is more specifically measured through patch-clamp experiments, high-throughput patch-clamp experiments require highly specialized equipment. Therefore, as in many ion channel assay platforms, we sought to employ a fluorescent dye that would respond to changes in TRPM7 conductivity. In combined patch-clamp or other low-throughput platforms, TRPM7 Ca^{2+} conductance has been previously measured employing various fluorescent cation binding dyes,[12,25] commonly using the ratiometric properties of the Ca^{2+} binding dye fura-2.[26] Alternatively, TRPM7 conductance of Mn^{2+}, Co^{2+}, and Ni^{2+} has been measured, also in low throughput, as the quench of Ca^{2+}-independent fura-2 fluorescence.[12] Based on its facile TRPM7 permeability and high fura-2 binding affinity, Mn^{2+} conductance gives the largest TRPM7-mediated quench of fura-2 in TRPM7 overexpressing cells, prompting us to select Mn^{2+} as the quenching reagent for our HTS assay. Measuring TRPM7-mediated Mn^{2+} entry, rather than Ca^{2+}, affords other advantages, including (a) some potentially competing cation entry pathways (e.g., calcium-release activated calcium [CRAC] channels) are less permeable than TRPM7 to Mn^{2+}; (b) CRAC channel current can be further disconnected by avoiding Ca^{2+}-deficient assay conditions, which are needed for optimal measurement of Ca^{2+} influx; and (c) the assay can be conducted in the presence of physiological levels of Ca^{2+} and Mg^{2+}.[12]

This article describes the development and optimization of a 96-well plate HTS assay that measures TRPM7-mediated Mn^{2+} influx in stably transfected HEK293 cells where the overexpression of the TRPM7 gene is under the control of an inducible promoter.[4] The expression of TRPM7 in these cells was confirmed by immunofluorescence and whole-cell current recordings, and the quality of the bioassay window for each experiment was evaluated based on its Z' factor value. The assay was validated by measuring the effects of known (nonselective) inhibitors, and assay performance was evaluated in a pilot scale screening of a marine microbial extract library.

MATERIALS AND METHODS

Solutions and chemicals

Cell culture media included fetal bovine serum (FBS; Mediatech, Manassas, VA), Dulbecco's modified Eagle's medium (DMEM; Mediatech), L-glutamine (Fisher, Pittsburg, PA), blasticidin (Invitrogen, Carlsbad, CA), zeocin (Invitrogen), and/or penicillin-streptomycin (Sigma, St. Louis, MO). A stock solution of tetracycline (Sigma) was prepared in water (1.0 mg/mL). Poly-L-lysine (70-150 kDa; Sigma) was dissolved (0.2 mg/mL) in phosphate buffer (1.4 mM NaCl, 27 mM KCl, 100 mM Na_2HPO_4, 20 mM KH_2PO_4 [pH 7.4]). Cell-based assays were performed in Krebs-Ringer-HEPES (KRH) buffer (135 mM NaCl, 5 mM KCl, 1.5 mM $MgCl_2$, 1.5 mM $CaCl_2$, 20 mM HEPES, 5.6 mM glucose). Fura-2 acetoxymethyl ester (fura-2-AM; Calbiochem, San Diego, CA) was dissolved in DMSO

to make 1-mM stock solutions and stored in the dark at –20 °C. The anion pump inhibitor probenecid (Sigma) was prepared fresh daily in 1 N NaOH to make a working solution of 500 mM, and the detergent pluronic F-127 (Sigma) was dissolved in methanol (MeOH) to make a 20% (w/v) stock solution, stored in the dark. TRPM7 inhibitors 2-APB (Sigma) and $LaCl_3$ (Sigma) were prepared fresh daily as 50-mM working solutions: 2-APB was dissolved in MeOH and $LaCl_3$ in water. $MnCl_2$ (Sigma) was dissolved in water to make a 1-M stock solution that was made fresh weekly. All chemicals were diluted to their desired concentrations in KRH except for $MnCl_2$, which was diluted in Ca^{2+}-free KRH. For patch-clamp experiments, cells were kept in standard external Ringer's solution (140 mM NaCl, 2.8 mM KCl, 1.0 mM $CaCl_2$, 2.0 mM $MgCl_2$, 11 mM glucose, 10 mM HEPES-NaOH [pH 7.2], 310 mOsm). Standard internal pipette-filling solutions contained 140 mM Cs-glutamate, 8.0 mM NaCl, 1.0 mM $MgCl_2$, and 10 mM HEPES (pH 7.2 adjusted with CsOH/KOH). Intracellular Ca^{2+} was buffered with 10 mM BAPTA. All aqueous solutions were autoclaved or sterile filtered immediately after preparation.

Cell culture

Wild-type (nontransfected) human embryonic kidney (WT-HEK293) cells and tetracycline-inducible HEK293 cells, stably transfected with a FLAG-murine TRPM7/pCDNA4/TO construct (TRPM7-HEK293),[4] were cultured in a humidified incubator, at 37 °C and 5% CO_2, in DMEM supplemented with 10% (v/v) FBS and 2 mM L-glutamine. Wild-type HEK293 culture medium was supplemented with 100 U/mL penicillin and 0.10 mg/mL streptomycin. TRPM7-HEK293 culture medium was supplemented with 5 μg/mL blasticidin and 0.4 mg/mL zeocin. Both cell lines tested negative for mycoplasma contamination (Cell Production Core Facility, University of Nebraska Medical Center, Omaha).

HTS assay for TRPM7 inhibitors

TRPM7 channel conductance was monitored using a FlexStation 3 scanning fluorometer (Molecular Devices, Sunnyvale, CA) to monitor the Ca^{2+}-independent (360-nm excitation/510-nm emission) fura-2 quench by Mn^{2+} in TRPM7 overexpressing HEK293 cells.[26] The FlexStation 3 measured the fluorescent signal intensity in relative fluorescence units (RFU), at 1.5-s intervals for 60 s, using a beam diameter of 1.5 to 2.0 mm. Following baseline measurements, Mn^{2+} was added extracellularly, and changes in cytosolic [Mn^{2+}] were monitored as the loss of relative fluorescence caused by fura-2 quenching. TRPM7-HEK293 cells (30,000, 60,000, or 120,000 cells/well) were plated in poly-L-lysine-coated, black clear-bottom 96-well plates (Greiner Bio-One, Monroe, NC). Subsequent TRPM7-expression was induced 2 to 3 h after plating by the addition of 1 μg/mL tetracycline. The culture medium was completely removed at 16 to 18 h postinduction and replaced with the following fura-2 loading buffer: KRH buffer supplemented with 0.5 to 4 μM fura-2-AM, with or without 2 mM probenecid, and with or without 0.1% to 0.3% pluronic F-127. Following variable incubation times (30, 45, and 60 min at 25 or 37 °C), the loading buffer was removed and replaced with assay buffer (KRH). The plates were then transferred to a room temperature (25 °C) or pre-warmed (37 °C) FlexStation, which also contained a clear V-bottom 96-well compound plate (Greiner Bio-One) with vehicle or appropriate test substance solutions diluted with KRH. Cells were initially incubated for 15 min with vehicle or test substance. Just prior to the addition of 1 or 10 mM $MnCl_2$, the baseline fluorescence was recorded for 20 s. The Ca^{2+}-independent, TRPM7-mediated fura-2 quench by Mn^{2+} was then recorded for 40 s.

Marine microbial extract library

Bacteria were isolated from marine sediments, sea water, and tissues of marine macroorganisms. The isolated bacteria were typed by GC fatty acid methyl ester analysis. For organisms unique to the collection, broth cultures (150 mL each) were prepared from 20% glycerol/media stocks using proprietary media that supports secondary metabolite production. Following incubation, the broth cultures were frozen, freeze-dried, and extracted with MeOH/dichloromethane (5:2). Extracts (n = 420) were plated in 96-well plates at 70 extracts/plate and stored as dry films. These plates are available from Magellan Bioscience Group, Inc. (Tampa, FL) as HPU_plates 14-16_21-23. Prior to testing in the optimized bioassay, extracts were redissolved in MeOH/ethyl acetate/*tert*-butyl methyl ether (60:30:10) (MET), diluted with KRH, and transferred by the FlexStation fluidics into assay plates at a final screening concentration of 100 μg/mL (n = 1, 2% MET). On each plate, positive vehicle controls (TRPM7-HEK293 cells, $n = 11_{c+}$) and background controls (WT-HEK293 cells, $n = 8_{c-}$) each received 2% MET. Threefold serial dilutions of 2-APB were included (n = 1 per concentration, 0.82-600 μM, ≤1.2% MeOH). Assay plates were preincubated with test substances for 15 min at 37 °C prior to addition of $MnCl_2$.

Electrophysiology

Patch-clamp experiments were performed in the whole-cell configuration at 24 °C. TRPM7-HEK293 cells were induced by 18-h exposure to 1 μg/mL tetracycline. Cells were kept in standard external NaCl-based solution containing 1 mM $CaCl_2$ and perfused with standard internal Cs-glutamate-based solution supplemented with 10 mM Cs-BAPTA. All data were acquired with PatchMaster (HEKA, Lambrecht, Germany) software controlling an EPC-9 amplifier (HEKA) and analyzed using FitMaster (HEKA) and IGOR PRO (Wavemetrics, Lake

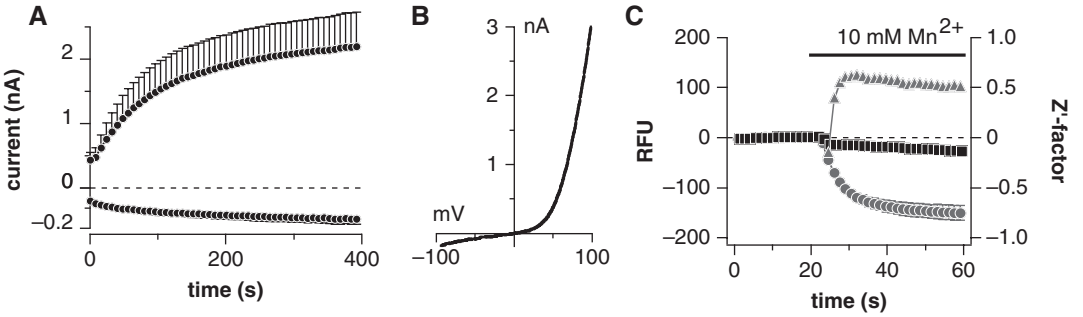

FIG. 1. Ionic current development and Mn^{2+}-induced fluorescent quench in HEK293-overexpressing mouse TRPM7. (**A**) Average time course of current development assessed in TRPM7-HEK293 using the whole-cell configuration of the patch-clamp technique (n = 10). Error bars indicate SEM. Note different scale for positive and negative currents. (**B**) Current-voltage (I/V) curve extracted from an example cell at 300 s into the whole-cell experiment. (**C**) Fura-2 quenching in TRPM7-HEK293 cells (positive control, blue circles) and noninduced TRPM7-HEK293 cells (negative controls, black circles) that were plated at 60,000 cells/well. The fura-2 loading buffer contained 2 μM fura-2-AM, 2 mM probenecid, and 0.1% pluronic F-127 in KRH, and incubation was at 37 °C for 60 min. Each data point is the mean ± SD of 48 replicate wells for TRPM7-HEK293 cells and 24 replicate wells for noninduced TRPM7-HEK293 cells, and Z′ factor values (red triangles) are plotted.

Oswego, OR). Voltage ramps of 50 ms spanning from –100 to +100 mV were delivered from a holding potential of 0 mV at a rate of 0.5 Hz. Voltages were corrected for liquid junction potentials (10 mV). Currents were filtered at 2.9 kHz and digitized at 100-μs intervals. Current amplitudes were extracted at +80 mV and –80 mV for analysis and display.

Statistical analysis

Fluorescence data were collected in SoftMax Pro (Molecular Devices) and processed in Microsoft Excel 2007. Replicate fluorescence traces (time vs. intensity) were averaged and the Z′ factors were calculated. Mean, standard deviation (SD), and Z′ factors (–1 to 1) at each time point were plotted using IGOR PRO (Wavemetrics). Data were routinely reduced (e.g., for determining percent inhibition and dose-response curves) by extracting endpoints at 10 s post-$MnCl_2$ addition. These values were background corrected (WT-HEK293 signal subtracted) and normalized to vehicle controls. IC_{50} curves for fluorescence-based HTS assays and whole-cell recordings were fitted by constraining the top of the curve (no inhibition) to 100% vehicle control in IGOR PRO.

RESULTS AND DISCUSSION

An inducible expression system for TRPM7 was chosen for the assay because stable overexpression leads to nonviable cell cultures due to cell detachment from the substrate and cell death.[4] At the same time, compared to transient transfection, the inducible expression system provides the additional advantage to be based on monoclonal cell selection and thereby ensures the highest uniformity of heterologous protein expression within the cell culture. Functional expression of FLAG-tagged murine-TRPM7 was demonstrated using the whole-cell configuration of the patch-clamp technique (**Fig. 1A**).[4] TRPM7 currents were recorded 18 h after tetracycline (1 μg/mL) induction and showed the typical behavior of strong outward current rectification (**Fig. 1A,B**). Induction beyond 20 h led to increased cell detachment, and therefore the induction period selected optimized TRPM7 expression level versus loss of cell adherence. Inducible overexpression of TRPM7 was also observed in the fluorescence bioassay by the significant difference between the magnitude of the fura-2 quench by Mn^{2+} when induced TRPM7-HEK293 cells and noninduced TRPM7-HEK293 cells were compared (**Fig. 1C**).[12] Furthermore, the quench of the fura-2 signal observed for noninduced TRPM7-HEK293 cells was comparable to that of WT-HEK293 cells (**Fig. 1C** vs. **Fig. 2B**). These results confirm that the quench of the fura-2 signal observed for induced TRPM7-HEK293 cells is not an artifact arising from the recombination process but is a result of TRPM7-mediated Mn^{2+} influx. Nevertheless, WT-HEK293 cells were selected as the background measurement for Mn^{2+} influx to avoid problems with variable response due to potential leaky TRPM7 expression in noninduced TRPM7-HEK293 cells. The use of a high concentration of La^{3+} or 2-APB on fully induced TRPM7-HEK293 cells was considered a background control, but due to the nonspecific inhibition of these agents, they hold the potential to overestimate the actual window of TRPM7-mediated Mn^{2+} influx.

The quality of the bioassay window was evaluated using the Z′ factor, a statistical parameter that is a measure of assay window quality for HTS.[27] The Z′ factor is defined by the following formula: $Z' = 1 - [3(SD_{c+} + SD_{c-})/(|mean_{c+} - mean_{c-}|)]$, where SD_{c+} and SD_{c-} are standard deviations for positive (TRPM7-HEK293 cells) and negative controls (WT-HEK293 cells), respectively, and $mean_{c+}$ and $mean_{c-}$ are the means for positive and negative controls, respectively. Similarly, the Z factor is a measure of an assay's

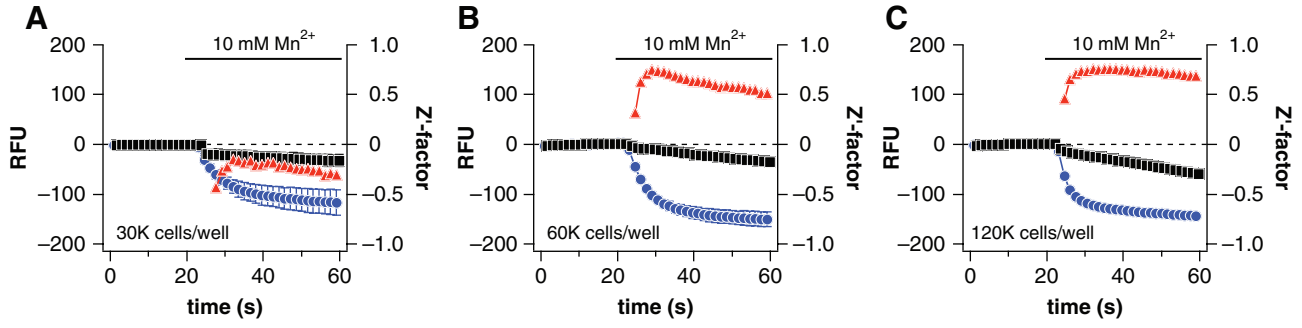

FIG. 2. Optimization of cell plating density. TRPM7-HEK293 cells (positive control, blue circles) and WT-HEK293 cells (negative controls, black squares) were plated at (**A**) 30,000, (**B**) 60,000, and (**C**) 120,000 cells/well. Each data point is the mean ± SD of 48 replicate wells for TRPM7-HEK293 cells and 24 replicate wells for WT-HEK293 cells, and Z′ factor values (red triangles) are plotted.

quality in HTS of a specific chemical library and reflects the influence of a compound library on assay performance. The Z factor is calculated for an inhibition assay by substituting the mean and standard deviation of the combined sample data for the $mean_{c+}$ and SD_{c+} in the above equation. Experiments with a Z/Z′ factor value ≥0.5 are considered to have an excellent assay window.[27]

In these analyses, the Z′ factor value was plotted together with the data representing the positive and negative controls. To make this graphical representation of assay window quality sensible, all error bars for data measurements represent the standard deviations mirroring the standard deviation's influence on the Z′ factor. Based on the Z′ factor value, the optimized bioassay demonstrates an excellent, reproducible assay window.

In many HTS platforms, the added step of media removal before experimentation comprises a major drawback,[28] especially when using nonadherent cell lines or cells that are prone to monolayer wash-off. In pilot experiments, we found for our bioassay that the use of poly-L-lysine-coated plates enhanced cell adherence and prevented wash-off, greatly improving the assay reproducibility. Our results demonstrate, as confirmed by the Z′ factor, that this bioassay successfully tolerates culture media removal before experimentation. Furthermore, by eliminating potential interactions between serum-containing, media, and test compounds, we reduce the likelihood of artifacts and false positives as well as false negatives.

The following conditions for the proposed bioassay were evaluated: (a) cell density, (b) dye loading concentration and incubation time, (c) presence of detergent and anion efflux pump inhibitor during dye loading, (d) bioassay temperature, (e) concentration of the fura-2 quenching agent Mn^{2+}, and (f) vehicle solvent concentrations. The bioassay was validated by calculating IC_{50} curves for the known TRPM7 inhibitors 2-APB and La^{3+}. The reproducibility of the proposed bioassay was measured by calculating Z′ factors for raw RFU data pooled from a single plate, between 2 plates assayed on the same day, and between 2 plates from separate days. To optimize cell density first, this study relied on experimental conditions that were iteratively derived from established lab protocols, literature values, and preliminary screenings. The same rationale was used for the fura-2-AM and $MnCl_2$ concentrations.

Optimization of cell density

TRPM7-HEK293 and WT-HEK293 were seeded at 30,000, 60,000, and 120,000 cells/well. Cells were incubated at 37 °C for 60 min with KRH containing 2 mM probenecid, 0.1% pluronic F-127, and 2 μM fura-2-AM. Cells seeded at 30,000 cells/well failed to demonstrate an acceptable assay window (**Fig. 2A**), whereas cells seeded at 60,000 cells/well and 120,000 cells/well demonstrated an excellent assay window (**Fig. 2B,C**, respectively). However, when cells were seeded at a density of 120,000 cells/well, the sheets of cell monolayers start to pile, which we found to be suboptimal for similar bioassay platforms in our lab because of problems with cell adhesion and nonlinear effects for the optics of the fluorescent readers. On this basis, we adopted the cell seeding density of 60,000 cells/well.

The use of alternate assay plates was not assessed, but we anticipate that this assay platform could be scaled to accommodate a 384-well plate format. Also, if a 96-well plate format is desirable, the consumption of expensive cell culture supplies and reagents as well as the amount of test compounds could be reduced by implementing the use of half-area 96-well plates. At the same time, we have optimized this bioassay using standard 96-well plates with cost efficiency in mind, using a final well volume of ~100 μL, which is an intermediate volume between that required for typical 96-well and 384-well plate assays.

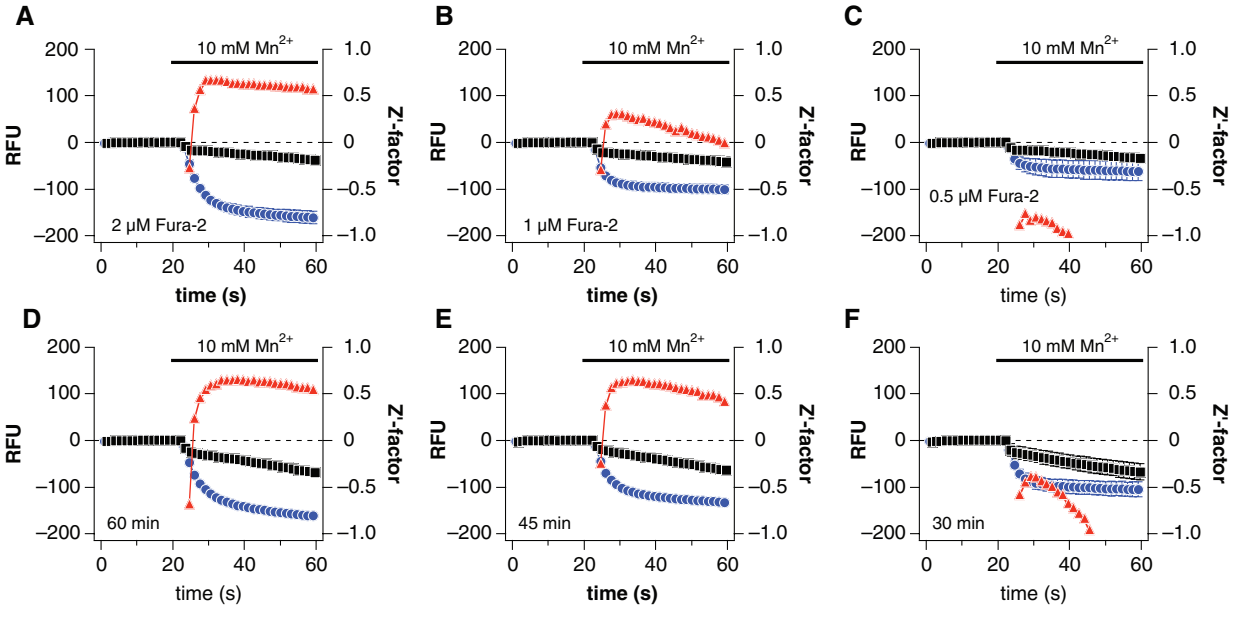

FIG. 3. Optimization of fura-2-AM concentration and loading time. TRPM7-HEK293 cells (positive control, blue circles) and WT-HEK293 cells (negative controls, black squares) were incubated with (**A**) 2 μM, (**B**) 1 μM, or (**C-F**) 0.5 μM fura-2-AM for (**A-D**) 60 min, (**E**) 45 min, or (**F**) 30 min prior to reading. Each data point is the mean ± SD of 48 replicate wells, and Z′ factor values (red triangles) are plotted.

Optimization of fura-2-AM concentration and loading time

TRPM7-HEK293 cells and WT-HEK293 cells were plated at 60,000 cells/well. Cells were incubated at 37 °C for 60 min with KRH containing 2 mM probenecid and 0.1% pluronic F-127 while varying the concentration of fura-2-AM between 0.5, 1, 2, and 4 μM. Following the addition of 10 mM $MnCl_2$, the fura-2-AM loading concentration of 2 μM fura-2-AM and 4 μM fura-2-AM both resulted in excellent assay windows (**Fig. 3A**; data not shown for 4 μM fura-2-AM). However, the loading concentration of 1 μM fura-2-AM and 0.5 μM fura-2-AM both failed to produce acceptable assay windows (**Fig. 3B,C**, respectively). The fura-2-AM loading concentration of 2 μM was selected for further optimization over 4 μM fura-2-AM as a compromise between the intensity of the signal (slightly larger signal and Z′ factor for 4 μM fura-2-AM) and cost efficiency (~$4.50/plate vs. ~$9.00/plate, respectively). Next, the effect of fura-2-AM loading time on the fluorescent signal given by the loading concentration of 2 μM fura-2-AM was investigated. For these experiments, the cells were loaded in KRH containing 2 mM probenecid, 0.1% pluronic F-127, and 2 μM fura-2-AM and were monitored after 60-, 45-, and 30-min fura-2-AM loading times. The 60- and 45-min fura-2-AM loading times both resulted in excellent assay windows (**Fig. 3D,E**, respectively). However, the 30-min fura-2-AM loading time failed to produce an acceptable assay window (**Fig. 3F**). Ultimately, the fura-2-AM loading time of 60 min was selected over 45 min based only on its better compatibility with the laboratory workflow.

Effects of probenecid (anion pump inhibitor) and pluronic F-127 (detergent) during fura-2-AM loading

TRPM7-HEK293 cells and WT-HEK293 cells were plated at 60,000 cells/well. Cells were incubated at 37 °C for 60 min with KRH containing 2 μM fura-2-AM, in the absence or presence of probenecid (2 mM) and pluronic F-127 (0.1%-0.3%). Following the addition of 10 mM $MnCl_2$, the data revealed that 2 mM probenecid had a stronger positive influence on assay window quality than did pluronic F-127 (**Fig. 4A,B**, respectively). Nevertheless, when pluronic F-127 was omitted (with probenecid present), a degradation in assay window quality was seen (**Fig. 4C**), indicating that both the anion pump inhibitor and the fura-2-AM solubilizing detergent work synergistically to produce excellent assay window quality. An increase in the concentration of pluronic F-127 (0.3%), in the presence of 2 mM probenecid, caused degradation in assay window quality (data not shown), and omitting both probenecid and pluronic F-127 resulted in unacceptable assay window quality (**Fig. 4D**).

Effects of temperature on fura-2-AM loading

TRPM7-HEK293 cells and WT-HEK293 cells were plated at 60,000 cells/well. Cells were incubated for 60 min with

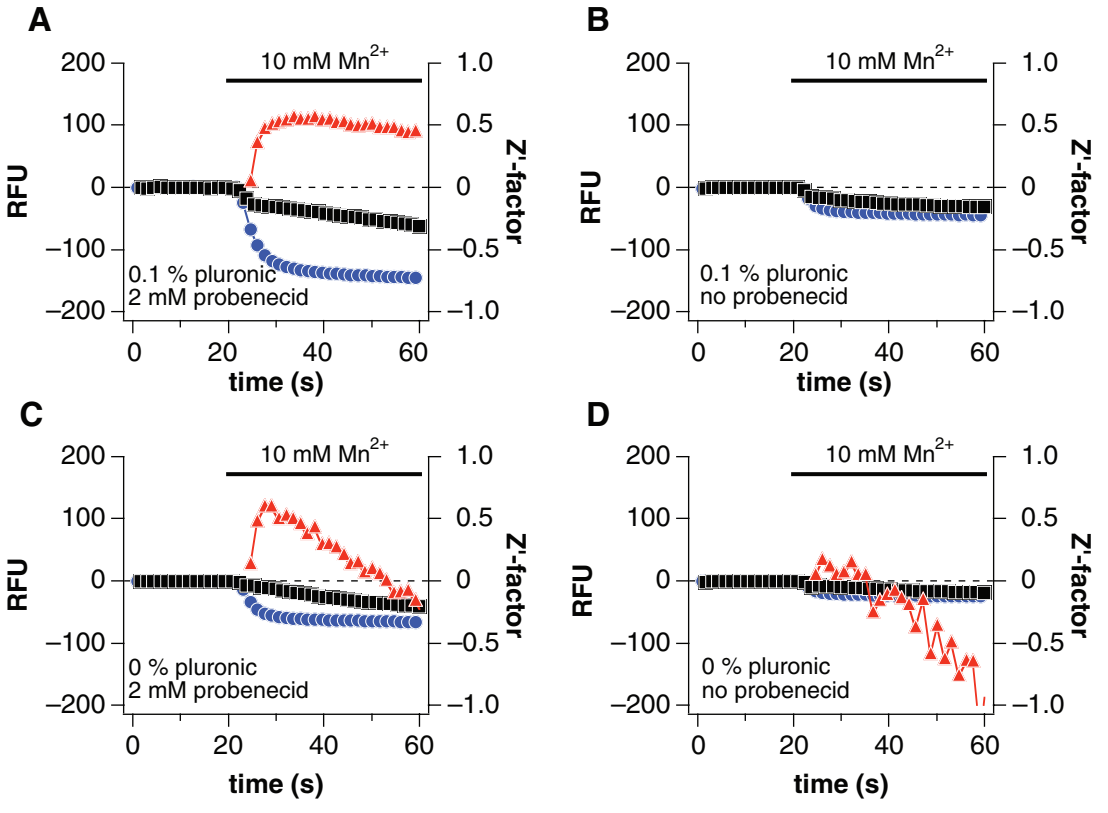

FIG. 4. Effects of probenecid and pluronic F-127 on fura-2-AM loading. TRPM7-HEK293 cells (positive control, blue circles) and WT-HEK293 cells (negative controls, black squares) were loaded with fura-2 in the presence of (**A**) 2 mM probenecid and 0.1% pluronic F-127, (**B**) 0.1% pluronic F-127 but without probenecid, (**C**) 2 mM probenecid but without pluronic F-127, or (**D**) no probenecid and no pluronic F-127. Each data point is the mean ± SD of 24 replicate wells for TRPM7-HEK293 cells and 12 replicate wells for WT-HEK293 cells, and Z′ factor values (red triangles) are plotted.

KRH containing 2 mM probenecid, 0.1% pluronic F-127, and 2 µM fura-2-AM while the temperature of incubation was either 25 °C or 37 °C. Following the addition of 10 mM $MnCl_2$, both fura-2-AM loading temperatures resulted in an excellent assay window quality (data not shown). We chose to use 37 °C as the loading temperature, being the more physiological temperature.

Concentration effects of extracellularly applied Mn^{2+} on assay window and kinetics

TRPM7-HEK293 cells and WT-HEK293 cells were plated at 60,000 cells/well. Cells were incubated at 37 °C for 60 min with KRH containing 2 mM probenecid, 0.1% pluronic F-127, and 2 µM fura-2-AM. The addition of 10 mM or 1 mM $MnCl_2$ (data not shown) both produced excellent assay window quality. Finally, we selected 10 mM $MnCl_2$ as the optimized parameter in favor of the observed larger signal magnitude and quicker kinetics.

Solvent tolerance

The solvent tolerance to 1% and 2% MeOH, DMSO, and MET was tested for the TRPM7-mediated fura-2 quench by Mn^{2+} in TRPM7-HEK293 and WT-HEK293 cells. Cells were plated at 60,000 cells/well and on the assay day were incubated at 37 °C for 60 min with KRH containing 2 mM probenecid, 0.1% pluronic F-127, and 2 µM fura-2-AM. After a wash step, the cells were preincubated with 1% and 2% MeOH, DMSO, and MET at 37 °C for 15 min, and the raw change in RFU (± SD) was analyzed ($n = 16_{c+,\,c-}$; 1% MeOH: $mean_{c+}$ –143.6 ± 5.4 RFU, $mean_{c-}$ –30.9 ± 2.3 RFU, Z′ factor 0.80; 2% MeOH: $mean_{c+}$ –147.2 ± 8.9, $mean_{c-}$ –30.7 ± 2.0 RFU, Z′ factor 0.72; 1% MET: $mean_{c+}$ –136.6 ± 6.1 RFU, $mean_{c-}$ –33.0 ± 6.2 RFU, Z′ factor 0.65; 2% MET: $mean_{c+}$ –147.8 ± 5.3, $mean_{c-}$ –29.2 ± 3.1 RFU, Z′ factor 0.79; 1% DMSO: $mean_{c+}$ –128.9 ± 8.8 RFU, $mean_{c-}$ –50.2 ± 4.0 RFU, Z′ factor 0.51; 2% DMSO: $mean_{c+}$ –147.1 ± 4.2 RFU, $mean_{c-}$ –67.1 ± 3.3 RFU, Z′ factor 0.72). The bioassay tolerated both concentrations of all 3 solvents,

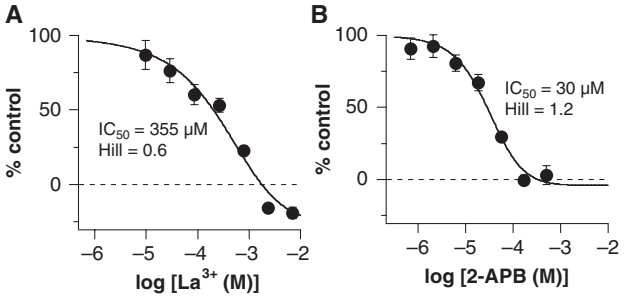

FIG. 5. Validation of the TRPM7-mediated fura-2 Quench by Mn^{2+}. TRPM7-HEK293 cells (positive control) and WT-HEK293 cells (negative controls) were preincubated with known nonselective inhibitors. (**A**) $LaCl_3$ was serial diluted 2:1 to give final concentrations of 7 mM to 9.6 µM, and each data point represents the mean ± SD of 8 replicate wells from 2 experiments. (**B**) 2-APB was serial diluted 2:1 to give final concentrations of 500 to 0.69 µM, and each data point represents the mean ± SD of 10 replicate wells from 2 experiments. The positive controls (n = 17) and negative controls (n = 16) on each plate, for each experimental day, yielded Z′ factors ≥0.5.

yielding an excellent assay window quality for each solvent concentration. We selected MET as our routine solvent based on its noninterfering nature in several of our bioassay systems, its documented superiority for compound storage,[29] and its ability to dissolve complex natural product extracts.

Assay validation

To validate the bioassay, we evaluated the effects of 2 known nonselective TRPM7 inhibitors, $LaCl_3$ and 2-APB. TRPM7-HEK293 cells and HEK293 cells were plated at 60,000 cells/well. Cells were incubated at 37 °C for 60 min with KRH containing 2 mM probenecid, 0.1% pluronic F-127, and 2 µM fura-2-AM. After a wash step, the cells were preincubated with $LaCl_3$ or 2-APB at 37 °C for 15 min during baseline measurements. Both $LaCl_3$ (**Fig. 5A**) and 2-APB (**Fig. 5B**) showed dose-dependent inhibition of the TRPM7-mediated fura-2 quench by Mn^{2+}. For La^{3+}, it was previously shown that inward TRPM7-mediated currents are almost completely blocked by 10 mM La^{3+}, whereas 10 µM La^{3+} is ineffective at blocking channel conductance.[12] Comparable results were obtained in the proposed bioassay where La^{3+} inhibited the TRPM7 channel with an IC_{50} value of 355 µM. In whole-cell current recordings using TRPM7-HEK293 and CHOK1-TRPM7 cells, 2-APB inhibited the TRPM7-mediated outward current with an IC_{50} value of 178 ± 14 µM.[20] It was also recently reported, in whole-cell current recordings using TRPM7-HEK293 cells, that 100 µM 2-APB inhibited the TRPM7-mediated inward current, in divalent-free extracellular solutions, by 77%.[15] In our hands, 2-APB showed dose-dependent inhibition of the TRPM7-mediated fura-2 quench by Mn^{2+} with an IC_{50} value of 30 µM.

It should be noted that proper compound treatment of 2-APB in solution was essential for accurate IC_{50} value determination. We observed that cold storage of 2-APB stock solutions (–20 °C, 50 mM in MeOH) resulted in apparent compound degradation over the course of 1 week, observed as a consistent increase in measured IC_{50} values. In addition, even dried-film, vacuum-packed aliquots of 2-APB, stored at –20 °C, only remained fully potent when used within a 2-month period. The method of compound storage may contribute to slight discrepancies between literature values and our values. Another possible contributing factor to the differences between our IC_{50} determinations and those aforementioned is that cells in this study were preincubated with $LaCl_3$ or 2-APB for 15 min prior to Mn^{2+} addition, which allows for an equilibration of slow kinetic processes. In contrast, simultaneous application of the channel inhibitors and channel recordings tends to underestimate the potency of "slow" inhibitors. In any case, given the experimental differences (drug application and fluorescent vs. electrophysiological readouts), the measured IC_{50} values remain quite comparable.

Assay reproducibility

TRPM7-HEK293 cells and WT-HEK293 cells were plated at 60,000 cells/well, and experiments were conducted at 18 h postinduction. Cells were incubated at 37 °C for 60 min with KRH containing 2 mM probenecid, 0.1% pluronic F-127, and 2 µM fura-2-AM. Following the addition of 10 mM $MnCl_2$, means ± SD were calculated using data points extracted from an endpoint 10 s after $MnCl_2$ addition. The reproducibility of the bioassay was measured by calculating Z′ factors for raw RFU data (± SD) pooled from a single plate (well-to-well reproducibility, $n = 48_{c+,\,c-}$, $mean_{c+}$ –109.8 ± 6.6 RFU, $mean_{c-}$ –30.5 ± 6.4 RFU, Z′ factor 0.51), between 2 plates assayed on the same day (plate-to-plate reproducibility, $n = 96_{c+,\,c-,}$ $mean_{c+}$ –107.3 ± 7.0 RFU, $mean_{c-}$ –29.5 ± 6.2 RFU, Z′ factor 0.49), and between 2 plates from separate days (day-to-day reproducibility, $n = 96_{c+,\,c-}$, $mean_{c+}$ –105.3 ± 5.4 RFU, $mean_{c-}$ –28.3 ± 5.0 RFU, Z′ factor 0.59). In each case, the Z′ factor was excellent, indicating that the assay is highly reproducible.

Pilot screening of a natural product library

A small library composed of extracts of marine bacterial cultures was screened to evaluate the performance of the assay for our intended use as an HTS for natural product libraries. Extracts (100 µg/mL) and 2-APB (3-fold serial dilutions) were tested in singlet on 6 assay plates and normalized to controls. The average IC_{50} value ± SD for 2-APB (n = 6, 63 ± 18 µM) was consistent with our previously measured potency (i.e., **Fig. 5B**). Pooled normalized controls indicated an excellent Z′ factor for the screen (**Fig. 6A**). Collective normalized extract responses were similar to positive controls, resulting in a Z factor

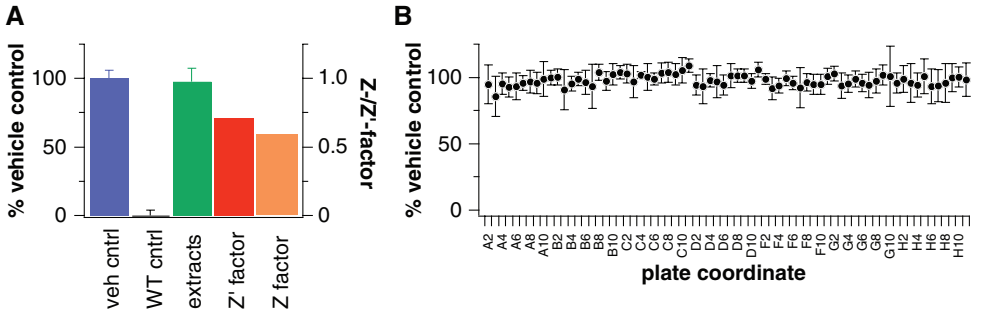

FIG. 6. Pilot screening of a marine-derived natural product library using the optimized TRPM7 assay. (**A**) TRPM7-HEK293 cells were preincubated with vehicle (positive control; $n = 66$) or microbial extracts (100 µg/mL; $n = 420$). WT-HEK293 cells were preincubated with vehicle (negative controls; $n = 48$). The Z′ factor was calculated from pooled normalized controls (± SD), and collective normalized extract responses were similar to positive controls and were used to calculate the Z factor. (**B**) Well-by-well pooled normalized extract responses ($n = 6$/well; ± SD).

of 0.59 (**Fig. 6A**). A well-by-well comparison of pooled extract data ($n = 6$ extracts/well; **Fig. 6B**) indicates consistent responses across the plate. No inhibitors were detected within the pilot library, which should not be surprising given the relatively small number of extracts. These data indicate that the assay performance is excellent in the context of relevant concentrations of complex natural product mixtures.

To summarize, we have developed and optimized a robust HTS bioassay capable of detecting TRPM7 inhibitors. In addition to comparing Mn^{2+} conductance in our TRPM7-HEK293 clones when induced versus noninduced, we confirmed the inducible expression of TRPM7 using functional expression by whole-cell patch-clamp experiments. We validated that our assay measures TRPM7-mediated conductance by evaluating the potencies of two known (nonselective) pharmacological inhibitors, which were comparable with published data for the same TRPM7 clone. Last, the performance of the assay was excellent against a pilot-scale natural product extract library.

The bioassay described here is, to our knowledge, the only reported HTS assay that measures the fluorescence quench of fura-2, rather than using the dye as a ratiometric intracellular Ca^{2+} indicator. This method could be adapted to other ion channel bioassays for HTS in which the selectivity profile of the ion channel of interest is matched to a fluorescent dye amenable to quenching by a permeating ion. In addition, the proposed bioassay holds great potential for advancing the understanding of TRPM7's physiological role and for validating the channel's role as a target in ischemic stroke and cell proliferative diseases. In addition to its use in screening chemical libraries, this assay can also be used to guide fractionation of active mixtures (e.g., natural product extracts or combinatorial samples) and evaluate relative potencies of synthetic products in lead compound optimization.

ACKNOWLEDGMENTS

We thank Dione Gray, Alex Pawlowski, and Stephanie Johne for excellent technical support and Jonathan Riel for valuable contributions to the optimization of the TRPM7 assay during the early phase of the project. We thank Drs. John Cronan and Todd Daviau from Magellan BioScience Group, Inc. (Tampa, FL) for kindly providing a marine microbial extract library in 96-well plates. We thank Dr. Yongli Chen for critical feedback. This work was supported in part by NIH P01GM078195 (AF), NIH R01GM080555 (RP), and NIH P20 RR-016467 (FDH).

REFERENCES

1. Nilius B, Owsianik G, Voets T, Peters JA: Transient receptor potential cation channels in disease. *Physiol Rev* 2007;87:165-217.
2. Ramsey IS, Delling M, Clapham DE: An introduction to TRP channels. *Annu Rev Physiol* 2006;68:619-647.
3. Desai BN, Clapham DE: TRP channels and mice deficient in TRP channels. *Pflugers Arch* 2005;451:11-18.
4. Nadler MJ, Hermosura MC, Inabe K, Perraud AL, Zhu Q, Stokes AJ, et al: LTRPC7 is a MgAtp-regulated divalent cation channel required for cell viability. *Nature* 2001;411:590-595.
5. Runnels L, Yue L, Clapham D: TRP-PLIK, a bifunctional protein with kinase and ion channel activities. *Science* 2001;291:1043-1047.
6. Fonfria E, Murdock PR, Cusdin FS, Benham CD, Kelsell RE, McNulty S: Tissue distribution profiles of the human TRPM cation channel family. *J Recept Signal Transduct Res* 2006;26:159-178.
7. Penner R, Fleig A: The Mg^{2+} and Mg^{2+}-nucleotide-regulated channel-kinase TRPM7. *Handb Exp Pharmacol* 2007;(179):313-328.
8. Demeuse P, Penner R, Fleig A: TRPM7 channel is regulated by magnesium nucleotides via its kinase domain. *J Gen Physiol* 2006;127:421-434.
9. Ryazanova LV, Pavur KS, Petrov AN, Dorovkov MV, Ryazanov AG: Novel type of signaling molecules: protein kinases covalently linked with ion channels. *Mol Biol* 2001;35:321-332.
10. Dorovkov MV, Ryazanov AG: Phosphorylation of annexin I by TRPM7 channel-kinase. *J Biol Chem* 2004;279:50643-50646.
11. Clark K, Middelbeek J, Lasonder E, Dulyaninova NG, Morrice NA, Ryazanov AG, et al: TRPM7 regulates myosin IIa filament stability and protein localization by heavy chain phosphorylation. *J Mol Biol* 2008;378:790-803.

12. Monteilh-Zoller MK, Hermosura MC, Nadler MJS, Scharenberg AM, Penner R, Fleig A: TRPM7 provides an ion channel mechanism for cellular entry of trace metal ions. *J Gen Physiol* 2003;121:49-60.
13. Aarts M, Iihara K, Wei WL, Xiong ZG, Arundine M, Cerwinski W, et al: A key role for TRPM7 channels in anoxic neuronal death. *Cell* 2003;115:863-877.
14. Jiang H, Tian SL, Zeng Y, Li LL, Shi J: TrkA pathway(s) is involved in regulation of TRPM7 expression in hippocampal neurons subjected to ischemic-reperfusion and oxygen-glucose deprivation. *Brain Res Bull* 2008;76:124-130.
15. Wei WL, Sun HS, Olah ME, Sun X, Czerwinska E, Czerwinski W, et al: TRPM7 channels in hippocampal neurons detect levels of extracellular divalent cations. *Proc Natl Acad Sci USA* 2007;104:16323-16328.
16. Sun HS, Jackson MF, Martin LJ, Jansen K, Teves L, Cui H, et al: Suppression of hippocampal TRPM7 protein prevents delayed neuronal death in brain ischemia. *Nat Neurosci* 2009;12:1300-1307.
17. Kim BJ, Park EJ, Lee JH, Jeon JH, Kim SJ, So I: Suppression of transient receptor potential melastatin 7 channel induces cell death in gastric cancer. *Cancer Sci* 2008;99:2502-2509.
18. Guilbert A, Gautier M, Dhennin-Duthille I, Haren N, Sevestre H, Ouadid-Ahidouch H: Evidence that TRPM7 is required for breast cancer cell proliferation. *Am J Physiol Cell Physiol* 2009;297:C493-C502.
19. Jiang J, Li MH, Inoue K, Chu XP, Seeds J, Xiong ZG: Transient receptor potential melastatin 7-like current in human head and neck carcinoma cells: role in cell proliferation. *Cancer Res* 2007;67:10929-10938.
20. Li M, Jiang J, Yue L: Functional characterization of homo- and heteromeric channel kinases TRPM6 and TRPM7. *J Gen Physiol* 2006;127:525-537.
21. Jiang X, Newell EW, Schlichter LC: Regulation of a TRPM7-like current in rat brain microglia. *J Biol Chem* 2003;278:42867-42876.
22. Inoue K, Xiong Z: Silencing TRPM7 promotes growth/proliferation and nitric oxide production of vascular endothelial cells via the ERK pathway. *Cardiovasc Res* 2009;83:547-557.
23. Parnas M, Peters M, Dadon D, Lev S, Vertkin I, Slutsky I, et al: Carvacrol is a novel inhibitor of drosophila TRPL and mammalian TRPM7 channels. *Cell Calcium* 2009;45:300-309.
24. Kozak JA, Matsushita M, Nairn AC, Cahalan MD: Charge screening by internal pH and polyvalent cations as a mechanism for activation, inhibition, and rundown of TRPM7/MICchannels. *J Gen Physiol* 2005;126:499-514.
25. Abed E, Labelle D, Martineau C, Loghin A, Moreau R: Expression of transient receptor potential (TRP) channels in human and murine osteoblast-like cells. *Mol Membr Biol* 2009;26:146-158.
26. Grynkiewicz G, Poenie M, Tsien Y: A new generation of Ca^{2+} indicators with greatly improved fluorescence properties. *J Biol Chem* 1985;360:3440-3450.
27. Zhang JH, Chung TD, Oldenburg KR: A simple statistical parameter for use in evaluation and validation of high throughput screening assays. *J Biomol Screen* 1999;4:67-73.
28. Song Y, Buelow B, Perraud AL, Scharenberg AM: Development and validation of a cell-based high-throughput screening assay for TRPM2 channel modulators. *J Biomol Screen* 2008;13:54-61.
29. Waybright TJ, Britt JR, McCloud TG: Overcoming problems of compound storage in DMSO: Solvent and process alternatives. *J Biomol Screen* 2009;14:708-715.

Address correspondence to:
Andrea Fleig
The Queen's Medical Center
1301 Punchbowl Street, Honolulu, HI 96813

E-mail: afleig@hawaii.edu